Appl Phys A (2010) 99: 549–556
DOI 10.1007/s00339-010-5672-6

Applied Physics A
Materials Science & Processing

Engineering the residual stress state and microstructure of stainless steel with mechanical surface treatments

M. Turski · S. Clitheroe · A.D. Evans · C. Rodopoulos · D.J. Hughes · P.J. Withers

Received: 30 March 2009 / Accepted: 24 February 2010 / Published online: 11 May 2010

Abstract Four mechanical surface treatments have been considered for the application to austenitic stainless steel structures. Shot peening (SP), laser shock peening (LSP), ultrasonic impact treatment (UIT) and water jet cavitation peening (WJCP), also known as cavitation shotless peening (CSP), have been applied to 8 mm thick Type 304 austenitic stainless steel coupons. This study considers the merits of each of these mechanical surface treatments in terms of their effect on the surface roughness, microstructure, level of plastic work and through thickness residual stress distribution. Microstructural studies have revealed the formation of martensite close to the treated surface for each process. Residual stress measurements in the samples show compressive stresses to a significantly greater depth for the LSP, UIT and WJCP samples compared to the more conventional SP treated sample.

1 Introduction

The fatigue loading or stress corrosion cracking responses of engineering components and structures are significantly influenced by the surface roughness, residual stress and degree of plastic work [1]. Surface stress engineering processes aim to improve the life of components through the generation of favourable compressive residual stress fields by locally plastically deforming the near surface region. The plastic deformation is associated with an indentation process arising from physical impingement and/or shockwaves from the surface treatment. The interplay between the residual stress field, the plastic strain and associated surface roughening from the process determines the effectiveness of the treatment [2]. Peening is the most common means of surface stress engineering to prolong life. Of the many peening methods shot peening is the most prevalent. This involves bombarding the surface with hard spherical media, each impact event generating an indent. Simplistically, the indentation process can be thought of as compressive plastic straining normal to the surface and tensile plastic straining parallel to the surface. This creates a local misfit with respect to the unstrained material, normally beneath this near surface region. The elastic response to the inhomogeneous plastic straining is thus the generation of in-plane compressive residual stresses near surface balanced by tensile residual stresses beneath. The associated surface roughening from the indentation process can be detrimental in terms of providing sites for crack initiation. Therefore, it is important that peening methods are optimised to improve the depth of favourable compressive residual stress fields while minimising surface roughening. This has driven the emergence of competitive processes to challenge shot peening. This paper compares shot peening with three such emerging techniques which exhibit favourable attributes. Laser shock peening (LSP) has seen increasing application in the aerospace and marine industry since the availability of fast repetition rate high power lasers [3]. Other candidate treatments include ultrasonic impact treatment (UIT) [4] and water jet cavitation peening (WJCP), also known as cavitation shotless peening

M. Turski (✉) · S. Clitheroe · P.J. Withers
School of Materials, Manchester University, Grosvenor St, M1 7HS, Manchester, UK
e-mail: mark.turski@magnesium-elektron.com

A.D. Evans
Paul Scherrer Institut, Villigen-PSI, 5232, Switzerland

C. Rodopoulos
University of Patras, Patras, Greece

D.J. Hughes
Institut Laue Langevin, Grenoble, 38042, France

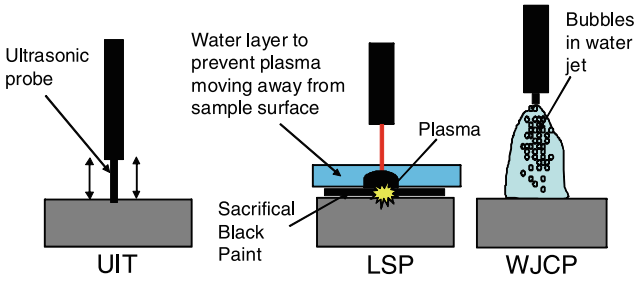

Fig. 1 Schematic description of the surface treatment process for ultrasonic impact treatment (UIT), laser shock peening (LSP), and water jet cavitation peening (WJCP)

(CSP) [5–7] (see Fig. 1). In this paper, each of these four peening methods is compared in terms of the residual stress depth profile, microstructure, surface roughness and plastic work.

Schematics for UIT, LSP and WJCP are depicted in Fig. 1. Typically, shot peening produces compressive residual stress to depths of between 100 and 500 μm accompanied by high levels of cold work (15–40%) [8]. In UIT, a high-frequency acoustic force (20–30 kHz) is applied, often by means of a portable tool, to the surface in order to introduce beneficial compressive stresses [4, 9]. LSP involves the generation of plastic deformation to the surface layers through laser-driven shock waves, generating compressive residual stresses to up to several millimetres in depth. The shock waves are produced from the confined, rapid expansion of a plasma generated by the irradiation of the surface (with or without a sacrificial coating) by a high power laser pulse [3, 10, 11]. The effectiveness of LSP for steels has been demonstrated through preventive maintenance against stress-corrosion cracking in operating nuclear power reactors since 1999 [12]. In WJCP, ultra-high pressure water jets are used to create a cloud of intense cavitation bubbles. Whether produced by flow or ultrasonically, cavitation introduces residual compressive stresses when the bubbles collapse on the surface producing a stress wave which plastically deforms the surface layers [5]. WJCP has been successfully applied to improve fatigue in aluminium alloys [6] and steels [7].

2 Experimental method

2.1 Specimen preparation

Specimens of 50 × 50 × 8 mm were produced for this peening study. Samples for UIT, LSP and WJCP were machined from the centre of a 12 mm thick 304 austenitic stainless steel plate, samples for SP were cut from a 304 L austenitic stainless steel 50 × 8 mm flat bar. The difference between 304 L and 304 stainless steel is very slight with the 304 alloy containing up to 0.05 wt% more carbon than the 304 L alloy. While this difference can affect corrosion resistance, it is not expected to significantly influence the material response to peening treatments. After cutting and machining, all samples were subsequently stress relieved to minimise the presence of any rolling or machining induced residual stresses. Stress relief treatment was carried out in an argon gas environment at 1050°C for 30 minutes. The furnace was heated at 20°C/minute and cooled using an argon gas fan quench.

2.2 Mechanical surface treatment

For each treatment two different levels of peening "intensity" were compared, in order to determine the sensitivity to peening strength.

2.2.1 Shot peening

Shot peening was carried out by the Metal Improvement Company, UK. The coupons were peened with hard steel shot up to 200% coverage. The first coupon was treated with S-110 shot grade to an Almen intensity of between 0.010 to 0.014". The second coupon was treated with S-330 shot grade, to the same Almen intensity. The shot grade describes the size of the shot media in ten-thousandths of an inch. In general terms, one would expect the larger shot radius to increase the depth of the compressive residual stresses. Peening was carried out over the entire coupon surface.

2.2.2 Laser shock peening

The LSP was performed at the Metal Improvement Company facility in Earby, UK. Samples were clamped against a backing plate and a water film run over the surface during laser shock peening. Prior to peening, the sample surface was covered with a sacrificial adhesive metal layer, which was removed after peening. The laser beam was oriented at 87°(almost normal) to the sample surface. The samples were treated with a laser power of 10 GW/cm^2, an 18 ns pulse width, laser fluence of 180 J/cm^2 and a spot size of 3 × 3 mm. Samples designated for low intensity treatment were laser peened with 2 layers, with each laser spot of the 2nd layer offset by 50%, thus ensuring complete coverage. Samples designated for high intensity treatment were laser peened with 3 layers. Peening was carried out to within 5 mm from the edge of the coupon leaving a constraining non-plastically deformed border.

2.2.3 Ultrasonic impact treatment

UIT was carried out at the University of Patras, Greece. The samples were treated with an ultrasonic transducer with a respective pin length and diameter of 35 and 6.3 mm. During their treatment, the transducer was translated along the

surface in a rastering motion at a speed of 150 mm/min. The level of peening intensity was controlled by changing the weight applied by the transducer pin. Samples designated for low intensity treatment were treated with an applied weight of 10 kg, while samples designated for the high intensity treatment were treated with an applied weight of 22 kg. UIT was carried out over the entire coupon surface, rastering the probe in a pattern of overlapping lines over the surface.

2.2.4 Water jet cavitation peening

WJCP was carried out at the Tohoku University, Japan. Samples were all treated using a tank pressure of 0.32 MPa, a nozzle diameter of 2 mm, an injection pressure of 30 MPa and a nozzle standoff distance of 80 mm. The low intensity peened sample was treated for the duration of 2 minutes and the high intensity peened sample was treated for 4 minutes. Peening was carried out at one position, resulting in a single annular treated region.

2.3 Specimen sectioning

With the exception of the WJCP samples, each treated plate was sectioned after peening to produce a number of samples for further investigations. Each sample was first sectioned into quarters using wire electro discharge machining (WEDM). A further 3 mm thick slice specimen was subsequently cut using WEDM from the inside face of each of the sectioned quarters. This produced a total of four $19 \times 19 \times 8$ mm and eight $19 \times 8 \times 3$ mm samples from each peened sample.

3 Characterisation of mechanical surface treated samples

3.1 Surface roughness and metallography

The surface roughness of each coupon was measured prior to sectioning. The surface roughness was measured using a μScan surface laser scanner produced by Nanofocus scanned using a 20×100 μm step size. Optical microscopy was performed on a through-thickness section of material, close to the centre plane of the coupon. Samples were prepared in the conventional manner using silicon carbide grit discs, followed by diamond polishing cloths. Samples were etched using 50% nitric acid and 50% water for 1 minute with a low applied voltage. The micrographs presented here correspond to the low intensity LSP and UIT, and high SP and WJCP treatments.

3.2 Quantification of plastic work

The depth and magnitude of plastic work (equivalent true strain) generated by the mechanical surface treatments were estimated using X-ray diffraction for the UIT, SP and LSP samples. This was achieved by correlating the full width at half maximum (FWHM) of the diffraction peak to calibration samples that have been uniaxially strained to known levels of equivalent true strain. The peak broadening (FWHM) of the peened samples was measured as a function of depth along with the plastically strained samples on the high resolution powder diffraction beamline ID31 at the ESRF, Grenoble, France. The experiments were performed at an X-ray energy of 60 keV which permitted transmission measurements to be made on 3 mm slices cut from the $25 \times 25 \times 8$ mm coupons. The incident beam was 200×200 μm, giving the spatial resolution in depth from the treated surface. The FWHM was measured as a function of depth from the treated surface for four lattice reflections. Within this paper, we will focus on the (311) reflection since this was the reflection used for residual stress studies using neutron diffraction. Measurements were also made on a set of calibration samples extracted from unpeened 304 stainless steel uniaxial tensile test specimens strained to 1, 2, 4, 7, 10, 14 and 18% true strain. These samples had been machined from a stress relieved, 20 mm thick plate.

3.3 Residual stress studies

Residual stress studies were performed on $19 \times 19 \times 8$ mm samples sectioned from the original coupons. The residual stresses were determined from lattice strains measured on the SALSA neuron diffractometer at the ILL, Grenoble, France [13]. Lattice strain was measured using the (311) reflection since it has been reported that it does not accumulate large intergranular stresses and is recommended for FCC materials by the standard for neutron scattering ISO/TTA 3:2001. The wavelength used was 1.655 Å giving a diffraction angle around 90° for the (311) reflection. The sampling gauge volume was defined in the horizontal plane by oscillating radial collimators and vertically by cadmium masks directly attached to the surface of the sample. This was done to ensure that only the treated region was sampled and not the surrounding border of undeformed material. Residual strains were calculated using a stress free lattice spacing, d_0, which was taken as an average through the bulk of an identical untreated annealed 304 coupon. The spurious strains associated with the near surface measurements (the initial 1 mm depth) were determined in the annealed d_0 plate by scanning through the near surface region. The plate was rotated 180° and the procedure repeated. The average of the two curves revealed negligible in-plane strains and was used for the empirical correction of the peening

residual strain profiles. The shot peened residual stresses were calculated assuming isotropic plane stress whereas the other samples were treated as anisotropic. Residual stresses were calculated using the diffraction elastic constants of E of 183.5 GPa and ν of 0.29 for the (311) reflection.

4 Results and discussion

4.1 Surface roughness

Figure 2 shows photographs of each surface treatment, it is clear that each peening treatment produces a characteristic surface texture. The SP treatment gives rise to a dimpled surface finish, while the UIT sample surface is significantly furrowed. These furrows are due to the dragging of the tool tip along the surface during peening, and are approximately 1 mm deep and 2 mm wide. The furrowing is usually mitigated by peening the sample in a cross-hatching fashion. The LSP produced the smoothest finish, with a characteristic patchwork pattern related to the incident laser beam spot size and impact pattern. The WJCP surface shows the original milled surface finish of the sample along with a portion of the annular peened region. The surface of the WJCP region is slightly rougher than the SP surface, and is pitted in nature, showing signs of surface erosion.

4.2 Near surface microstructure

Figure 3 shows representative microstructures for each of the peening treatments. All four systems show evidence of deformation induced martensite (DIM) apparent as thin linear directional striations retained within grains. DIM is observed over a depth of 100 μm for the SP sample. By contrast, for the three other processes the effect is observed to several hundred microns, although not homogeneously. Transformation of austenite to martensite is known to occur due to deformation of austenitic stainless steels [14]. For 304 stainless steels, studies have been carried out on the effects of strain rate, grain size and stress state [15] on the level of DIM. Varma et al. measured DIM on samples deformed by uniaxial tensile testing at strain rates of 5, 0.5 and 0.01/min and found higher levels of DIM for larger grain sizes; however, no correlation was found between volume fraction of DIM and strain rate [15]. This suggests that the plastic work calibration samples (see Sect. 3.2) could contain DIM. Varma et al. also found a correlation between the stress state and the amount of DIM formed, higher levels were found during rolling than uniaxial loading, suggesting the formation of DIM is favoured during multiaxial loading [15]. The microstructures in Fig. 3 also show a shallow grain refined band close to the sample surface, due to severe plastic deformation in this region. The presence of DIM has been reported for deep rolling treatment of 304 stainless steel [16]; however, none was observed for LSP for the reported process parameters [16]. Investigations on 321 stainless steel by Mordyuk et al. observed DIM in ultrasonically peened samples but not for LSP samples [17]. The absence of martensite was attributed to the temperature increase generated by the ablation process [17]. The presence of DIM found in the LSP sample examined in this paper may be attributed to the use of a metallic protective tape combined with a film of running water during peening. The presence of the tape and water is believed to prevent localised heating during the LSP process. No mention of the use of a protective metallic film or water could be found in the LSP process parameters described in [16] or [17]. The susceptibility of a given stainless steel alloy to DIM is thought to be related to the stacking fault energy (SFE) [18]. Alloys with a low SFE, such as 304 stainless steel, would be expected to form DIM more readily than stainless steels with a high SFE, such as 316 stainless steel.

4.3 Residual stress

The residual stress profiles presented in Figs. 4 show that while all the surface treatments studied generate near surface compressive residual stresses, the depths to which they extend, and their magnitudes near surface, differ appreciably.

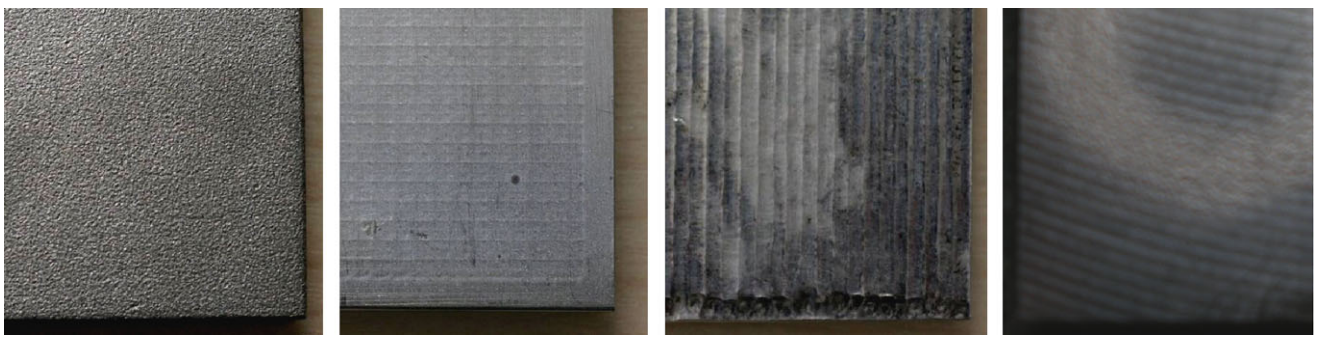

Fig. 2 Photographs of peened surface for (from *left* to *right*) SP, LSP, UIT and WJCP. The area displayed in each case is approximately 25 × 25 mm

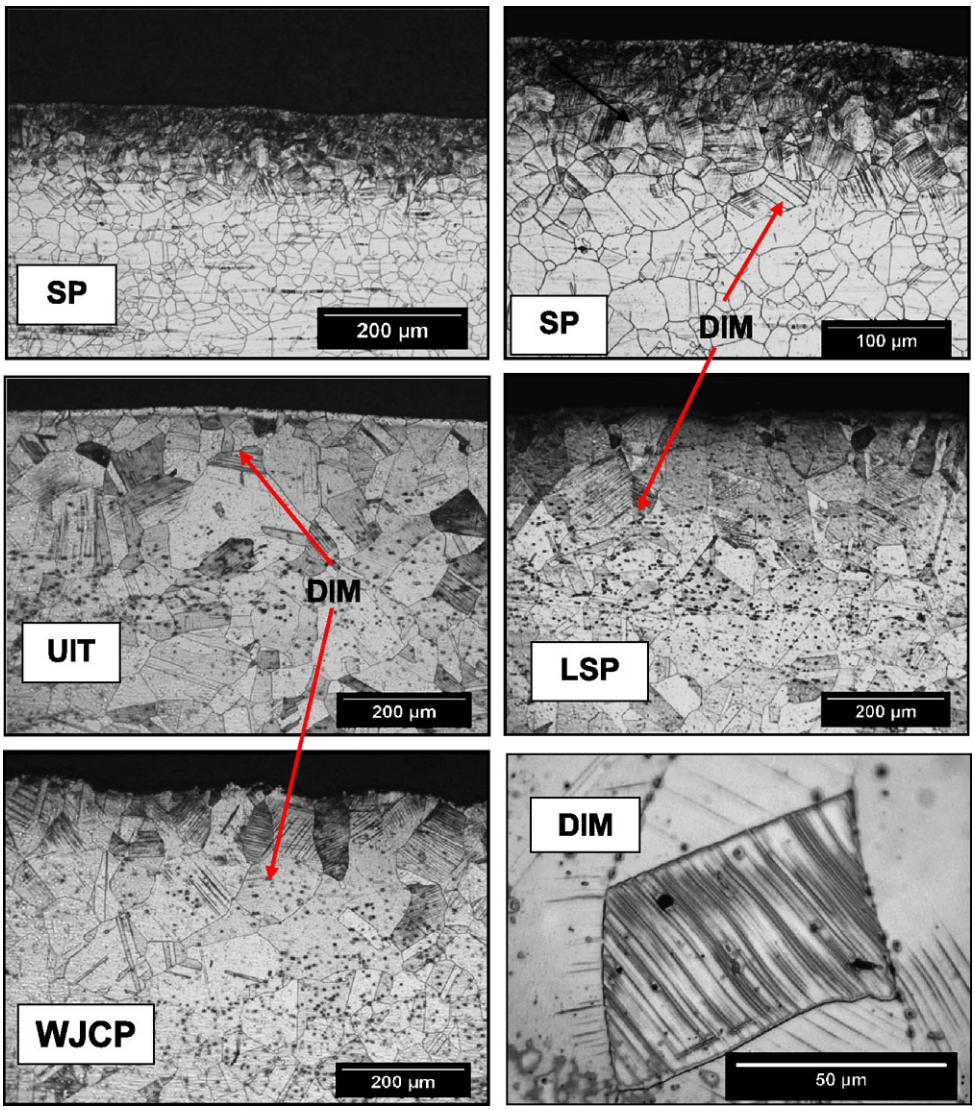

Fig. 3 Cross-sectional micrographs of the peened samples exhibiting deformation induced martensite

All the conditions generate an essentially linear stress profile beyond the plastically affected depth due to the elastic bending stresses generated by the treatment. This places the back surface in compression, and is similar in level for all the deep treatment methods (LSP, UIT and WJCP). The shot peening depth profiles (Fig. 4(a)), taken as the baseline for the comparison, exhibit a compressive residual stresses profile that is a maximum closest to the surface becoming tensile within 200 µm of the surface. The surface stress is greater than the static yield strength of the alloy, indicative of extensive work hardening. The other treatments exhibit an order of magnitude increase in the depth of compression compared to shot peening, however, the magnitudes of the surface compression in the case of LSP and WJCP are lower. Unsurprisingly, the presence of a deep layer of compressive residual stress generated by UIT, WJCP and in particular LSP appears to generate higher balancing tensile residual stresses compared to SP and more severe elastic bending in the remainder of the plate. Finally, while SP, LSP and WJCP introduce an isotropic in-plane residual stress state, UIT generates an anisotropic condition with the highest compression levels found perpendicular to the application direction of the tool. It should be noted that the presence of martensite in the initial 100 µm was not measured during the neutron diffraction measurements since only the (311) austenite reflection was recorded. For this reason, the residual stresses determined near the surface of each sample are only a representation of the stress within the austenite phase; however, the volume fraction of martensite is very low and so would not be expected to greatly influence the average stress in the austenite, even near surface. It is possible that the presence of martensite has changed the amount of carbon present in the austenite and thus the stress free lattice spacing (which were made within untreated 304 plate). However, in view of the low fraction of martensite, this is not expected to be significant.

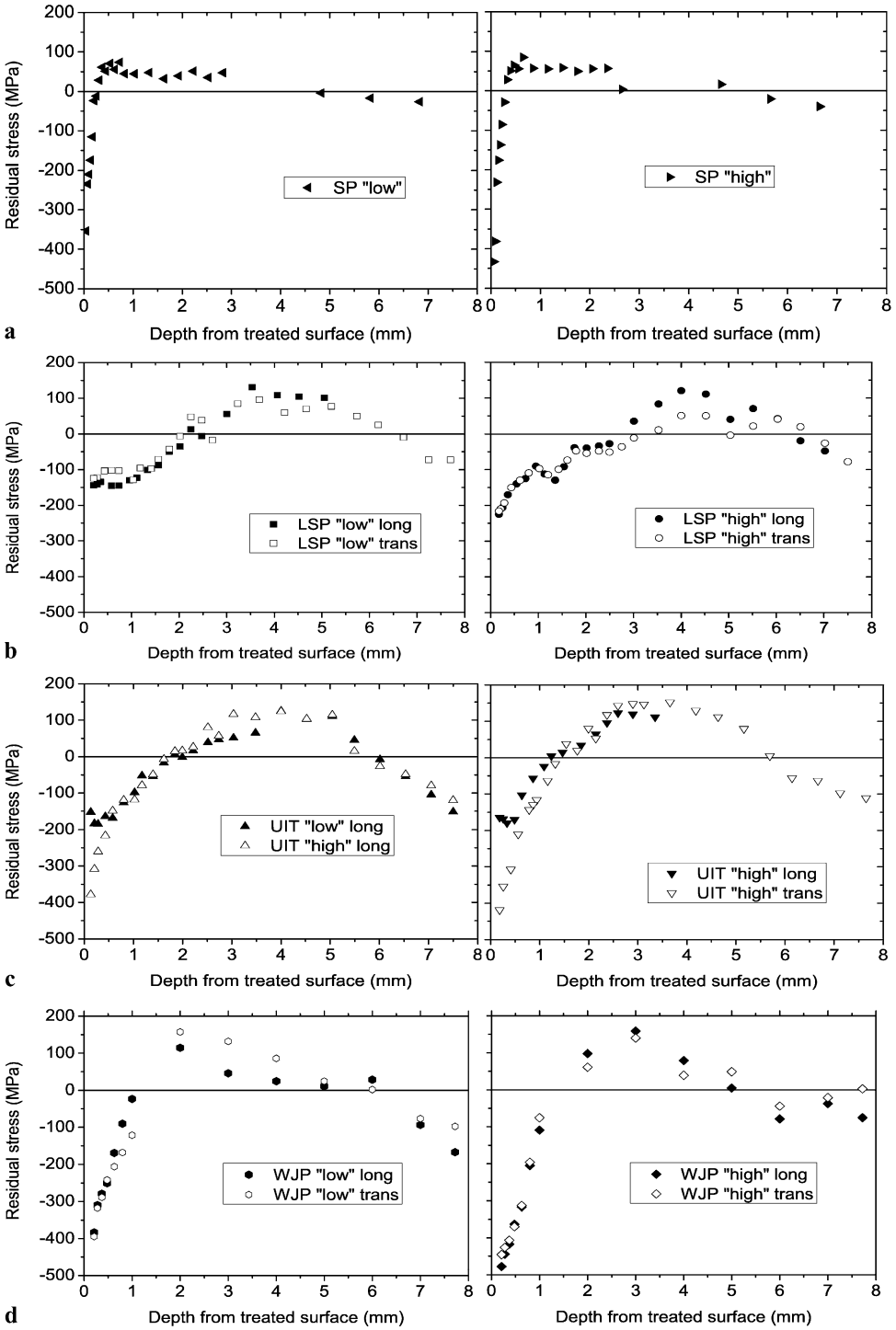

Fig. 4 Residual stress for low and high intensity surface treatments by (**a**) shot peening, (**b**) laser peening, (**c**) ultrasonic impact treatment, (**d**) cavitation peening as determined by neutron diffraction

4.4 Plastic work

The FWHM was correlated with plastic strain by plotting the measured FWHM against imposed plastic strain, as measured on the pre-strained coupons (see Fig. 5). The results show close agreement to a linear fit over the plastic strain range measured. This fit was used to estimate the level of plastic work as a function of depth from the treated surface for each of the peened samples. In this way, the FWHM measurements in the peened samples have been equated to an equivalent uniaxial plastic strain. This should be regarded as an approximate measure because the presence of a low level amount of martensite could increase the FWHM somewhat and thereby cause the inferred plastic strains to be an upper-bound. The FWHM and equivalent plastic strain for each of the peened samples have been plotted in Fig. 6. The plots

suggest peak levels of plastic work of about 12% for both UIT and LSP samples at the sample surface, reducing to the baseline values after 2 mm. The SP plots show much higher levels of plastic work near surface, with peak values of up to 23% at the sample surface, decaying to baseline values after 0.5 mm. This higher level of plastic work would explain the higher level of microstructural refinement observed at the surface of the SP samples in Fig. 3. The results also indicate that more plastic work is accumulated for the higher intensity peening parameters. However, the residual stress profiles in Fig. 4 indicate a negligible increase in magnitude or depth of compressive stress for the higher intensity peening parameters. This indicates that beyond a certain plastic strain, further increases only produce redundant plastic strain which does not lead to further increases in the level of residual stress. This can be understood using the concept of eigenstrain, where there is a geometrically necessary level of inelastic strain required to produce a certain elastic residual stress distribution. Further inelastic strains are impotent in the sense they do not generate increasing residual stress level but only redundant plasticity.

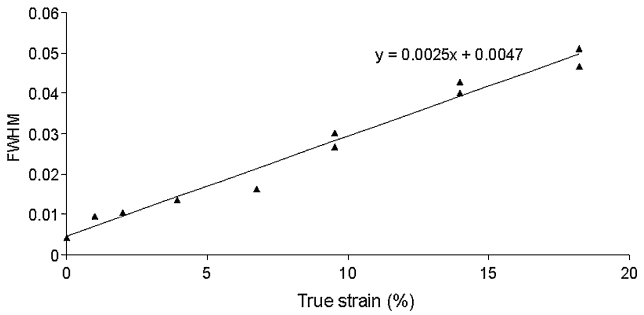

Fig. 5 Calibration plot of FWHM of the 311 crystal reflection versus true strain generated by uniaxial tensile loading

When considering these results, it should be borne in mind that the empirical measure of plastic strain presented here ignores the complex mechanics of the loading involved in the application of plastic strain by the treatment. It also neglects the cyclic nature of the loading of the certain treatments. Our measurement of the peak broadening captures qualitatively the contributions of modified crystallite size and root mean squared (rms) strains generated by the plastic deformation. Nevertheless, the high levels of inferred plastic strain near the surface are consistent with the presence of DIM induced martensite.

The concept of redundant plastic work in peening processes is of importance considering the evidence of increased susceptibility to stress corrosion cracking [19] and creep damage [20] with increasing cold work for austenitic stainless steels. For this reason, it may be desirable to limit the level of cold work while maximising the level of compressive stress. However, further work is required to fully understand the relationship between plastic work and material degradation mechanisms.

5 Summary

There are many reasons why a particular surface treatment is the preferred choice for a particular application. These include cost, ease of application in the field, surface finish, depth of compressive stress, repeatability of application, etc. In this paper, we have compared the efficacy of

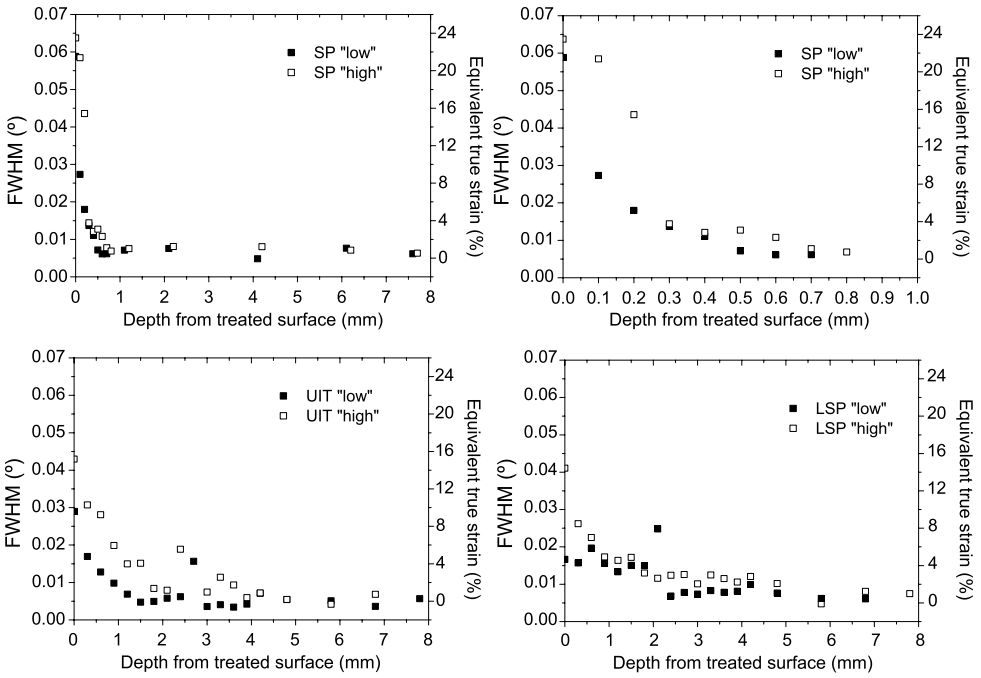

Fig. 6 The variation in diffraction peak full width half maximum measured for the (311) reflection measured on ID31 at the ESRF as a function of depth from the treated surface. The right-hand axis also denotes the equivalent plastic strain, as inferred from the calibration curve shown in Fig. 5

UIT, LSP and WJCP peening at introducing residual stresses and modifying the near surface state compared to the shot peening benchmark for 304 stainless steel. They all produce compressive residual stress fields to 1–2 mm compared to 200 μm for shot peening, although the magnitude just beneath the surface (∼100 μm) is somewhat lower for LSP using the applied processing parameters. Of the four methods WJCP and LSP introduced the lowest levels of surface roughening. In terms of near surface plastic work, diffraction peak broadenings suggest that the level of work introduced by LSP and UIT is considerably less than for shot peening, although the depth of work hardening extends to greater depths. In all cases, the plastic straining induced limited martensitic transformation at the surface. This may have important consequences for corrosion.

Acknowledgements The authors are grateful for assistance from Prof. Soyama for water jet cavitation peening and the Metal Improvement Company for shot peening and laser shock peening. Assistance with the diffraction measurements from Dr. Kelleher and Mr. Gonzalez are also acknowledged. The authors acknowledge access to diffraction facilities at the beamlines ID31, ID11 (ESRF) and (SALSA) ILL. Advice from Prof. T. Mori is also gratefully acknowledged.

References

1. H. Gray, L. Wagner, G. Lütjering, in *Proc. 3rd Int. Conf. on Shot peening (ICSP-3), Garmish-Partenhirchen, Germany*, ed. by H. Wohlfahrt, R. Kopp, O. Vöhringer (DGM Info. Verlag, Oberusel, 1987), pp. 447–458
2. S. Curtis, E.R. de los Rios, C.A. Rodopoulos, A. Levers, Int. J. Fatigue **25**(1), 59–66 (2003)
3. J.E. Masse, Surf. Coat. Technol. **70**, 231–234 (1995)
4. E. Statnikov, Ultrasonics **44**, 533–538 (2006)
5. H. Soyama, J.D. Park, M. Saka, J. Manuf. Sci. Eng **122**, 83–89 (2000)
6. H. Soyama, K. Saito, M. Saka, J. Eng. Mater. Technol. **124**, 135–139 (2002)
7. H. Soyama, T. Kusaka, M. Saka, J. Mater. Sci. Lett. **20**, 1263–1265 (2001)
8. W.Z. Zhuang, G.R. Halford, Int. J. Fatigue **23**, S31–S37 (2001)
9. L. Huo, D. Wang, Y. Zhang, Int. J. Fatigue **27**, 95–101 (2005)
10. A. King, A. Steuwer, C. Woodward, P.J. Withers, Mater. Sci. Eng. A **435–436**, 12–18 (2006)
11. B.N. Mordyuk, Yu.V. Milman, M.O. Iefimov, G.I. Prokopenko, V.V. Silberschmidt, M.I. Danylenko, A.V. Kotko, Surf. Coat. Technol. **202**, 4875–4883 (2008)
12. Y. Sano, M. Obata, T. Kubo, N. Mukai, M. Yoda, K. Masaki, Y. Ochi, Mater. Sci. Eng. A **417**, 334–340 (2006)
13. T. Pirling, G. Bruno, P.J. Withers, Mater. Sci. Eng. **437A**, 139–144 (2006)
14. A. Sato, Y. Sunaga, T. Mori, Acta Metall. **25**, 627 (1976)
15. S.K. Varma, J. Kalyanam, L.E. Murr, V. Shrinivas, J. Mater. Sci. Lett. **13**, 107–111 (1994)
16. I. Nikitin, B. Scholtes, H.J. Maier, I. Altenberger, Scr. Mater. **50**, 1345–1350 (2004)
17. B.N. Mordyuk, Yu.V. Milman, M.O. Iefimov, G.I. Prokopenko, V.V. Silberschmidt, M.I. Danylenko, A.V. Kotko, Surf. Coat. Technol. **202**(19), 4875–4883 (2008)
18. S.S.M. Tavaresa, J.M. Pardal, M.J. Gomes da Silvab, H.F.G. Abreub, M.R. da Silvac, Mater. Charact. **60**, 907–911 (2009)
19. C. García, F. Martín, P. De Tiedra, J.A. Heredero, M.L. Aparicio, Corros. Sci. **43**, 1519–1539 (2001)
20. M. Turski, P.J. Bouchard, A. Steuwer, P.J. Withers, Acta Mater. **56**, 3598–3612 (2008)